Limnol. Oceanogr., 56(4), 2011, 1463–1474

doi:10.4319/lo.2011.56.4.1463

Large ancient organic matter contributions to Arctic marine sediments (Svalbard)

J.-H. Kim,[a,*] F. Peterse,[a] V. Willmott,[a] D. Klitgaard Kristensen,[b] M. Baas,[a] S. Schouten,[a] and J. S. Sinninghe Damsté[a]

[a] Royal Netherlands Institute for Sea Research, Department of Marine Organic Biogeochemistry, Texel, The Netherlands
[b] Norwegian Polar Institute, Polar Environmental Centre, Tromsø, Norway

Abstract

Soils, fine-grained ice-rafted detritus (IRD), coals, and marine surface sediments in the Arctic realm (Svalbard) were collected in 2007 and 2008 to characterize organic matter (OM) sources in Arctic marine sediments. Bulk geochemical (C : N ratio and stable carbon isotopic composition) parameters suggest a predominant marine contribution to sedimentary OM. The branched and isoprenoid tetraether index (a proxy of soil OM input) indicates that soil OM contribution to the marine sediments is minor. However, the presence of retene (used as an indicator for coal-derived OM), the low carbon preference index and the average chain length of *n*-alkanes, and the depleted bulk radiocarbon content ($\Delta^{14}C$ value) suggest that ancient OM of both coal-derived and mature IRD-derived OM is being buried in the Kongsfjord–Krossfjord system of Svalbard in the high Arctic. The relatively low retene concentrations in the marine surface sediments other than those in close vicinity of Ny Ålesund, previously a coal-mining town, indicated that input of IRD-derived OM was predominantly responsible for the generally low $\Delta^{14}C$ value. We applied three-end-member models based on $\Delta^{14}C$ and retene and *n*-alkane concentration data to disentangle relative coal-derived, IRD-derived, and marine OM proportions to sedimentary OM. Sediments were comprised on average 2% ± 4% of coal-derived OM, 37% ± 17% of IRD-derived OM, and 61% ± 18% of marine OM with higher IRD-derived OM deposit in the Kongsvegen glacier front. Our results highlight the important role of ancient OM on carbon dynamics in Arctic environments, in particular for benthic food webs.

Permafrost soils in the Arctic regions store 23–48% of world's soil organic carbon (OC, Guo and Macdonald 2006). During spring–summer the upper soil layer above the permafrost thaws and a considerable portion of suspended and dissolved soil-derived OC may be transported with the large flux of freshwater from the continents into the Arctic Ocean (Macdonald et al. 1998). Part of the organic matter (OM), mainly suspended particulate OM, settles in the drainage areas and the Arctic rivers contain the highest OM concentrations in the world (Dixon et al. 1994). Dissolved and colloidal OM in these rivers is of modern origin, presumably from the leaching and decomposition of fresh plant litter in the upper soil horizons (Benner et al. 2004; Guo and Macdonald 2006; Neff et al. 2006). In contrast, particulate OM in these rivers have highly depleted $\Delta^{14}C$ values, likely from the input of recalcitrant, preaged soil OM and/or thermally matured ancient OM (Guo et al. 2004). Most of these Arctic rivers drain into the Arctic Ocean, which contains 20% of the world's continental shelf area (Macdonald et al. 1998). Numerous studies of the Arctic margins showed that estuarine and shelf sediments are dominated by terrestrial OM transported from land to coastal seas via Arctic rivers and coastal erosion (Yunker et al. 1995; Goñi et al. 2000; van Dongen et al. 2008). Sedimentary OM on the Arctic estuarine and shelf is substantially depleted in ^{14}C, suggesting that soil-derived or ancient OM forms a substantial fraction of the sedimentary OM (Goñi et al. 2005; Drenzek et al. 2007).

In recent years, the Kongsfjord–Krossfjord system of Svalbard in the high Arctic has received considerable attention as a high-latitude ecosystem model and a particularly suitable monitoring site for exploring the effect of possible climate changes, with Atlantic water influx and melting of tidal glaciers, both linked to climate variability (Hop et al. 2002; Svendsen et al. 2002; Wiencke 2004). Although the sheltered Kongsfjord–Krossfjord system is not in itself representative of the whole Arctic basin, this area is one of the most accessible Arctic environments, providing an ideal site for a long-term survey to study the responses of the Arctic system to anticipated further climate changes. Knowledge of OM dynamics in this system may improve parameterization of biogeochemical processes in the Arctic carbon cycle and the resulting whole ecosystem model can then be joined to climate models to make predictions concerning the effects of global warming on the Arctic marine ecosystem (Svendsen et al. 2002). Previous studies (Svendsen et al. 2002; Winkelmann and Knies 2005), although mostly based on bulk organic parameters such as the C : N ratio and the stable carbon isotopic composition of OC ($\delta^{13}C_{org}$), indicated that the sediments in the Kongsfjord–Krossfjord system contain marine-dominated OM. However, this approach does not allow constraints on specific contributions of soil and ancient OM (Dickens et al. 2004; Drenzek et al. 2007).

In this study, we applied the Branched and Isoprenoid Tetraether (BIT) index (Hopmans et al. 2004), a proxy of fluvial soil OM input to the ocean (Huguet et al. 2007; Walsh et al. 2008; Kim et al. 2009*a*), to estimate soil OM contribution in the Kongsfjord–Krossfjord system. To characterize the influx of terrestrial OM in the fjord system

* Corresponding author: Jung-Hyun.Kim@nioz.nl

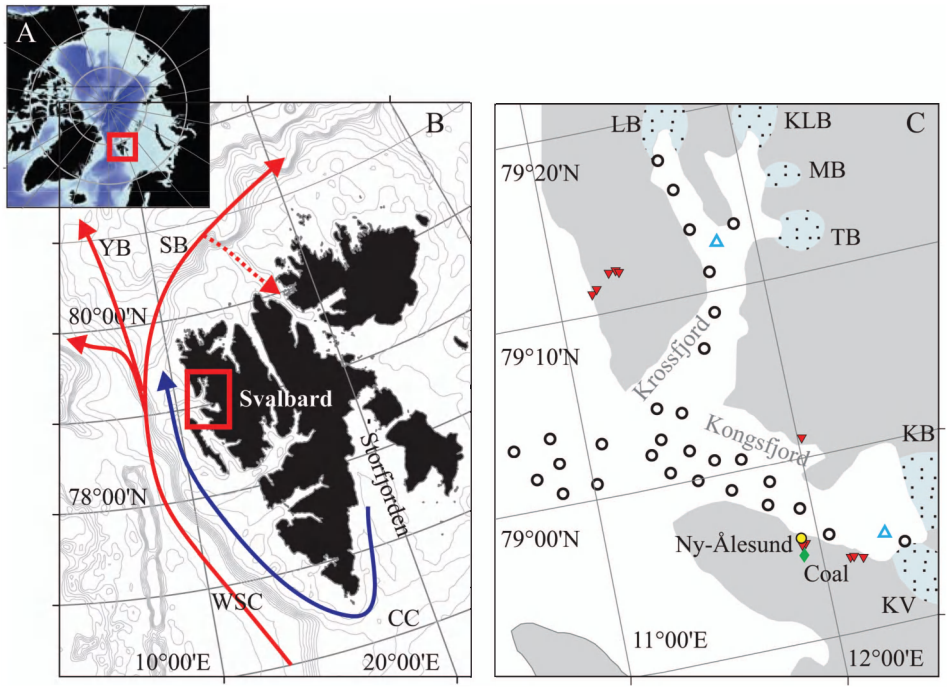

Fig. 1. (A) Map of the Arctic Ocean. (B) More detailed map of Svalbard with surface currents and the study area in red square. SB, YB, WSC, and ESC denote Svalbard Branch, Yermak Branch, West Spitsbergen Current, and East Spitsbergen Current, respectively. (C) Sampling locations of marine surface sediment in black open circles, IRD in blue open triangles, soil in red filled triangles, and coal in a green filled diamond. LB, KLB, MB, TB, KB, and KV indicate Lilliehöökbreen, Kollerbreen, Mayerbreen, Tinayrebreen, Kongsbreen, and Kongvegen, respectively.

and determine its contribution to OM in marine sediments, we also analyzed retene, 1-methyl-7-isopropyl phenanthrene (Simoneit et al. 1986; Grimalt et al. 1988), a compound formed upon maturation of higher plant triterpenoids. To further constrain the source of terrestrial OM, we analyzed *n*-alkanes derived from higher plant waxes (Eglinton and Hamilton 1963). To determine the influx of ancient radiocarbon-'dead' OM, we measured the radiocarbon content of OM ($\Delta^{14}C$). Our results give qualitative and quantitative assessments of OM source and composition in the Kongsfjord–Krossfjord system, highlighting a substantial contribution of ancient radiocarbon-dead OM to the present-day Arctic marine sedimentary OM pool.

Krossfjord–Kongsfjord system (Spitsbergen, Svalbard)

The Svalbard archipelago is situated in the high Arctic between 76°N and 81°N (Fig. 1A,B). The largest island of the archipelago is Spitsbergen, separated from the island Nordaustlandet by the Hinlopen Strait. Presently about 60% of the land is covered by glaciers and ice caps (Svendsen et al. 2002). The Kongsfjord–Krossfjord system is comprised of glacial, open Arctic fjords, and is located on the northwestern coast of Spitsbergen (78°40′–77°30′N and 11°3′–13°6′E). Kongsfjord is 20 km long and its width varies from 4 km to 10 km (Fig. 1C). Two glaciers, Kongsbreen and Kongsvegen, head the fjord. The scientific settlement, Ny-Ålesund (78°55′N and 11°56′E) is located on the southern shore of Kongsfjord and is one of only four permanent settlements on Spitsbergen. Krossfjord is 30 km long and its width varies between 3 km and 6 km. To the north it branches into Lillehöökfjord, Möllerfjord, and Kollerfjord. To the south it is separated from Kongsfjord by a line from Collinsodden on Mitrahalvøya east to Kapp Guissez. Lillehöökbreen glacier heads the Lillehöökfjord.

The climate of Svalbard is modulated by the West Spitsbergen Current (WSC; Fig. 1B), the northernmost extension of the North Atlantic Current, which brings heat and moisture to the region (Svendsen et al. 2002). Surface waters at the Spitsbergen continental margin are also characterized by colder Arctic waters (temperature < 0°C, salinity < 34.4; Loeng 1991). Common to high-latitude fjords, the hydrology of the study area is strongly influenced by freshwater inputs as meltwater from large tidal glaciers (Svendsen et al. 2002). The Kongsfjord–Krossfjord system experiences seasonality in the sea-ice cover, frozen during winter, but open under the influence of the ocean during summer. In recent years Kongsfjord has experienced a strong inflow of Atlantic water. This strong inflow has also affected the winter in Kongsfjord and has led to a strong reduction in sea-ice formation in the fjord (Cottier et al. 2007). Subglacial meltwater discharge from the tidewater glaciers is the main source of the sediment into the fjords. The sedimentation rate of silt–clay at the ice front is > 10 cm yr^{-1} (Svendsen et al. 2002). Ice melting during spring and summer creates a stratified and nutrient-

rich euphotic zone, which supports distinct plankton blooms along the ice margin (Owrid et al. 2000). Phytoplankton in fjord waters is dominated by diatoms and daily primary production is high during summer (Hop et al. 2002).

Methods

Sampling of soils, coals, ice-rafted detritus, and marine surface sediments—Eight soils around Krossfjord and Kongsfjord were collected during the SciencePub International Polar Year (IPY)-cruise (NP-08-16) in August 2008. In addition, we used data reported by Peterse et al. (2009), obtained from seven soils that were collected during the SciencePub IPY-cruise (NP-07-13) in September 2007 (Fig. 1C). Top-soils (i.e., upper 10-cm soils) were collected with a small scoop and stored in geochemical bags. In addition to the soils, three Tertiary coal samples collected around the former coal-mine village Ny Ålesund and the town of Longyearbyen were further investigated in this study. A fine-grained ice-rafted detritus (IRD) sample was collected from a drifting iceberg at the head of Krossfjord, as well as three IRD samples from different parts of an iceberg floating at the head of Kongsfjord during the NP-08-16 cruise.

In total, 29 multicores of marine sediments were collected aboard the R/V *Lance* during the SciencePub IPY-cruise (NP-07-13) in Krossfjord and Kongsfjord. The sediment cores were sliced at 1-cm interval and immediately deep-frozen at −20°C on board. All samples were transported to Royal Netherlands Institute for Sea Research and upon arrival at the laboratory kept at −40°C until further analyses. They were freeze-dried and homogenized prior to analysis.

Elemental and stable isotope analysis—Total organic carbon (TOC) of decalcified sample, using 2 mol L^{-1} HCl, and total nitrogen (TN) of bulk material were analyzed with a Thermo Elemental Analyser Flash EA 1112. The analyses were performed in at least duplicate, and data are given in weight percentages (wt.%). The reproducibility of TOC and TN analyses for marine sediments is 0.03% and 0.01%, respectively, and for soils and IRD 0.5% and 0.03%, respectively.

After acidification of samples with 2 mol L^{-1} HCl, $\delta^{13}C_{org}$ was determined using a Flash EA 1112 Elemental Analyser interfaced with a ThermoFinnigan Delta^{Plus} mass spectrometer. Isotope values were calibrated to a benzoic acid standard ($\delta^{13}C = -27.8‰$ with respect to Vienna Pee Dee Belemnite [VPDB]), calibrated on NBS-22 (lubricating oil) and corrected for blank contribution. The $\delta^{13}C_{org}$ values are reported in the standard delta notation relative to VPDB standard. The analyses were done at least in triplicate and data reported represent the mean of these analyses. The analytical reproducibility was generally < 0.2‰.

Radiocarbon (^{14}C) analysis—Acceleration mass spectrometry (AMS) radiocarbon (^{14}C) analysis was performed on OC of four soils, two IRD samples, seven marine surface sediments, and a coal sample at Beta Analytic Radiocarbon Dating Laboratory in Miami, Florida. Radiocarbon results are presented in the Delta notation ($\Delta^{14}C$, ‰) as defined by Stuiver and Polach (1977) and include the $\delta^{13}C$ (‰ VPDB) correction obtained from the stable isotope results. The conventional ^{14}C age before present ('present' = AD 1950) were calculated using the Libby ^{14}C half-life (5568 yr). Percent modern values above 100 show incorporation of radiocarbon produced from the atmospheric testing of nuclear weapons (bomb-^{14}C) and, thus, unequivocally indicate contributions from carbon-synthesized post-AD 1950 (Levin and Hesshaimer 2000).

Lipid extraction and purification procedure—Samples (1–5 g) were extracted with an Accelerated Solvent Extractor using a mixture of dichloromethane (DCM) : methanol (MeOH; 9 : 1 v : v) at a temperature of 100°C and a pressure of 7.6×10^6 Pa. The supernatants were combined, the solvents were removed by rotary evaporation, and the extracts were taken up in DCM and dried over anhydrous Na_2SO_4. An internal standard, a C_{46} glycerol dialkyl glycerol tetraether (GDGT), for GDGT quantifications was added to the total extracts before they were separated into three fractions over an Al_2O_3 column (activated for 2 h at 150°C) using hexane : DCM (9 : 1 v : v), hexane : DCM (1 : 1 v : v), and DCM : MeOH (1 : 1 v : v), respectively.

Retene analysis—For the quantification of retene, a known amount of the deuterated *anteiso* C_{22} alkane was added to the hexane : DCM (9 : 1 v : v) fraction as an internal standard. To identify and quantify retene, the apolar fractions were analyzed with a Thermo Finnigan trace gas chromatograph (GC) equipped with an on-column injector and fitted with a fused-silica capillary column (25 m × 0.32 mm) coated with CP Sil 5 (film thickness 0.12 μm). The GC oven was heated from 70°C to 130°C at 20°C min^{-1}, followed by 4°C min^{-1} to 320°C (10-min holding time). The column was directly inserted into the electron impact ion of a Thermo Finnigan Dual-Stage Quadrupole mass spectrometer, scanning a mass range of m : z 40–800 at 3 scans s^{-1} and an ionization energy of 70 *e*V. Identification of retene is based on comparison of relative GC retention time and mass spectrum published in the literature. Retene is in low abundance and co-eluting with other compounds; therefore, its quantification was performed by integrating specific ion traces, m : z 57 for the deuterated *ante-iso* C_{22} alkane and m : z 234 for the retene derived from full-scan total ion current. Absolute concentrations were obtained by correcting the different ion contributions of the m : z 57 (19%) and m : z 234 (13%) to the total ion count of the deuterated *ante-iso* C_{22} alkane and the retene identified in the coal samples. This quantification approach is somewhat less precise that that using GC-FID (see below).

Aliphatic hydrocarbon analysis—For aliphatic hydrocarbon (*n*-alkane) analysis, the apolar fractions of the total lipid extracts (hexane : DCM, 9 : 1 v : v) were further purified over a $AgNO_3$ impregnated silica-gel column using hexane as eluent. Analyses were performed on a Agilent

Technologies 6890N series II gas chromatograph equipped with an on-column injector and fitted with a fused-silica capillary column (50 m × 0.32 mm) coated with CP Sil 5 (film thickness 0.12 μm). Helium was used as carrier gas. The GC oven was heated from 70°C to 130°C at 20°C min^{-1}, followed by 4°C min^{-1} to 320°C (25-min holding time). Effluents were detected using flame ionization (FID). Quantification of compounds was performed by peak area integration in FID chromatograms relative to those of the deuterated *ante-iso* C_{22} alkane internal standard. The carbon preference index (CPI; Bray and Evans 1961) and the average chain length (ACL; Poynter and Eglinton 1990) of *n*-alkanes were calculated as follows:

$$\mathrm{CPI} = \frac{1}{2} \times \left[\left(\frac{\mathrm{C25+C27+C29+C31}}{\mathrm{C24+C26+C28+C30}} \right) + \left(\frac{\mathrm{C25+C27+C29+C31}}{\mathrm{C26+C28+C30+C32}} \right) \right] \quad (1)$$

$$\mathrm{ACL} = \frac{(\Sigma(\mathrm{Ci}) \times \mathrm{i})}{\Sigma(\mathrm{Ci})} \quad (2)$$

where i is the range of carbon numbers (25–31) and Ci is the concentration of the *n*-alkane containing i carbon atoms.

GDGT analysis—The polar fractions (DCM : MeOH, 1 : 1; v : v) were analyzed for GDGTs according to the procedure described by Hopmans et al. (2000) and Schouten et al. (2007). Aliquots of polar fractions were dried down under nitrogen, redissolved by sonication (5 min) in hexane : propanol (99 : 1 v : v), and filtered through 0.45-μm polytetrafluoroethylene filters. The samples were analyzed using high-performance liquid chromatography–atmospheric pressure positive-ion chemical ionization mass spectrometry (HPLC–APCI-MS). GDGTs were detected by single-ion monitoring of their $(M+H)^+$ ions (dwell time 237 ms) and quantification of the GDGT compounds was achieved by integrating the peak areas and using the C_{46} GDGT internal standard according to Huguet et al. (2006). The BIT index was calculated according to Hopmans et al. (2004):

$$\text{BIT index} = \frac{[\mathrm{I}] + [\mathrm{II}] + [\mathrm{III}]}{[\mathrm{I}] + [\mathrm{II}] + [\mathrm{III}] + [\mathrm{IV}]} \quad (3)$$

I, II, and III are concentrations of branched GDGTs and IV the concentration of isoprenoid GDGT, crenarchaeol. The analytical error in the determination of the BIT index is, on average, 0.01.

Results

TOC, C : N ratio, and $\delta^{13}C_{org}$—The TOC content of soils examined in this study and those by Peterse et al. (2009) varied between 0.6 wt.% and 10 wt.% and the average TOC value was 3.1 ± 3.1 wt.% (n = 15). The C : N ratio, calculated as TOC : TN, ranged from 8 to 31 (average = 14.3 ± 5.7, n = 15) and $\delta^{13}C_{org}$ from −27.1 to −25.2‰ (average = −26.1 ± 0.6‰, n = 15). All the IRD samples had a TOC content of 0.1 wt.%, a C : N ratio ranging from 1 to 6 (average = 3.3, n = 4), and $\delta^{13}C_{org}$ varying between −23.8‰ and −20.3‰ (average = −22.6‰, n = 4). The coal samples had an average TOC content of 529 wt.% (n = 3) and an average $\delta^{13}C_{org}$ value of −25.0‰ (n = 3). The C : N ratio varied between 22 and 52. The TOC contents of marine surface sediments ranged from 0.2 wt.% to 2.3 wt.% (average = 1.4 ± 0.6 wt.%, n = 29), while the C : N ratio ranged from 5 to 9 (average = 7.6 ± 0.8, n = 29) and $\delta^{13}C_{org}$ from −23.6‰ to −21.0‰ (average = −22.3 ± 0.6‰, n = 29). The C : N ratio and $\delta^{13}C_{org}$ data are plotted in Figs. 2A,B; 3A,B.

Radiocarbon ($\Delta^{14}C$)—The $\Delta^{14}C$ values of soils varied between −354‰ and +107‰ with the soil sample collected in Ny Ålesund (NA1) having the lowest value (corresponding to 3.4 kyr BP). The signal of the coal sample was statistically indistinguishable from background (i.e., a $\Delta^{14}C$ value of −1000‰). The $\Delta^{14}C$ values of the two investigated IRD samples were heavily depleted at −756‰ (11.2 kyr BP) and −862‰ (15.7 kyr BP). The $\Delta^{14}C$ values of selected marine sediments were all depleted in ^{14}C and varied between −735‰ (10.5 kyr BP) and −203‰ (1.64 kyr BP). These data together with the $\delta^{13}C_{org}$ values are plotted in Fig. 4A.

Retene—As a marker for terrestrial OM, we analysed retene, which is an aromatic derivative of β-amyrin, a common plant triterpenoid, formed upon maturation (Simoneit et al. 1986; Grimalt et al. 1988). The retene concentration was normalized to TOC (μg g_{OC}^{-1}) to identify samples with a substantially increased retene input. Retene was detected in high amounts in the coal samples (average = 568 μg g_{OC}^{-1}, n = 3), while it was absent in all soils except those collected in the vicinity of Ny Ålesund, where concentrations ranged from 38 μg g_{OC}^{-1} to 590 μg g_{OC}^{-1}. Retene was not detected in IRD but was present in most of the marine surface sediments, ranging in concentration from 1 μg g_{OC}^{-1} to 91 μg g_{OC}^{-1} (average = 16 ± 21 μg g_{OC}^{-1}, n = 26). These data are plotted in Figs. 2C, 3C.

N-alkanes—A homologous series of long-chain *n*-alkanes (n-C_{22} to n-C_{33}) was detected in all investigated soils, IRD, marine sediments, and in the coal. The CPI and ACL values of the C_{25}–C_{31} *n*-alkanes of the soils ranged from 2 to 23 (average = 12.6 ± 6.5, n = 15) and from 27 to 30 (average = 29.0 ± 0.8, n = 15), respectively (Fig. 4B). For the IRD and marine sediments, the CPI values ranged from 2 to 6 (average = 5.0, n = 4) and from 1 to 2 (average = 1.4 ± 0.3, n = 29), while the ACL varied between 28 and 29 (average = 29.0, n = 4) and between 26 and 28 (average = 28.1 ± 0.2, n = 29), respectively. The coal samples had an average CPI value of 2 (n = 3) and an average ACL value of 27 (n = 3). The summed C_{25} to C_{31} *n*-alkane concentration (ΣALK_{25-31}) of the coal samples ranged from 202 μg g_{OC}^{-1} to 308 μg g_{OC}^{-1} (average = 263 μg g_{OC}^{-1}, n = 3), while that of soils varied between 190 μg g_{OC}^{-1} and 1100 μg g_{OC}^{-1} (average = 430 ± 240 μg g_{OC}^{-1}, n = 15). The *n*-alkane concentration of the

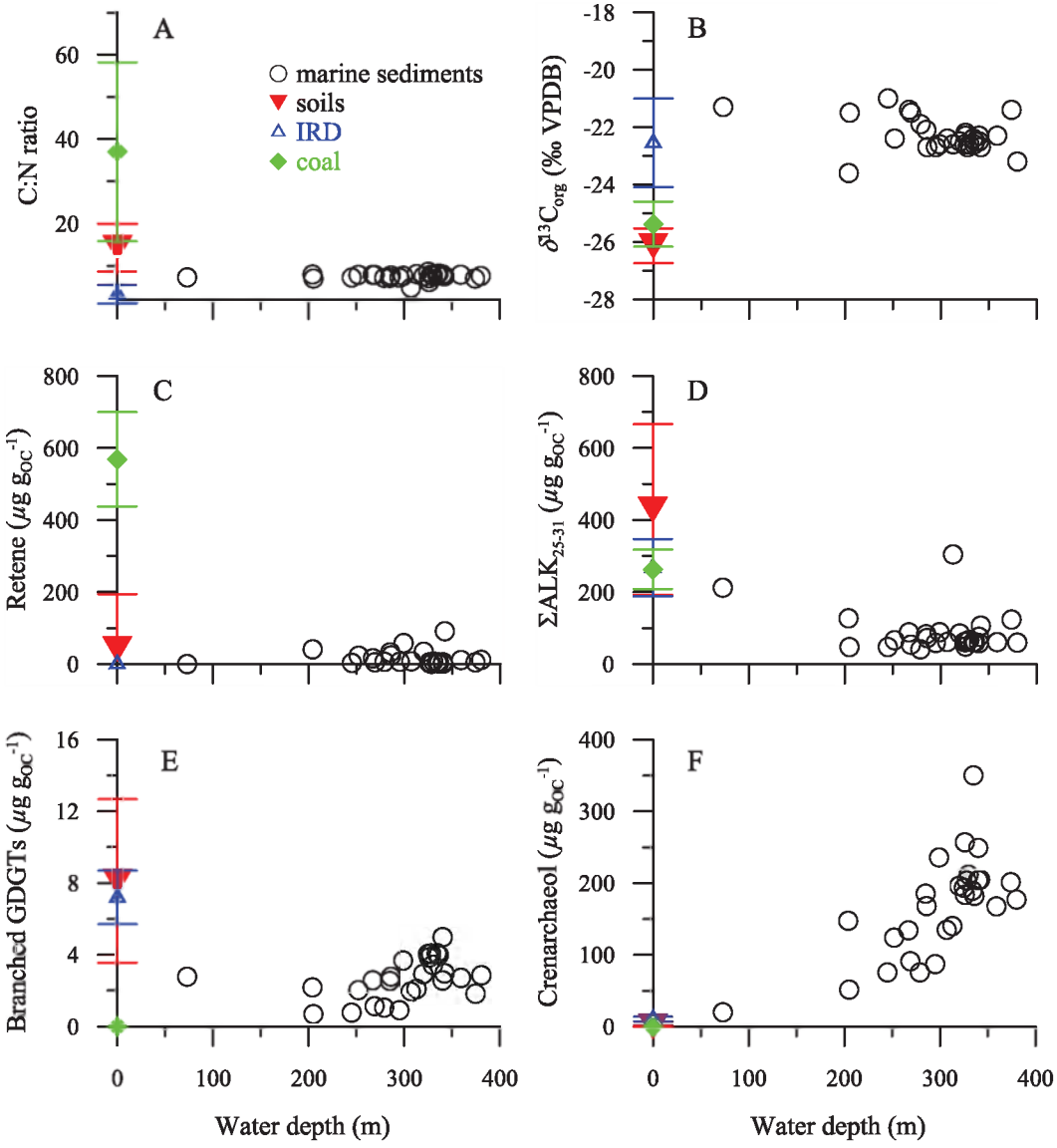

Fig. 2. Scatter-plot of water depth vs. (A) C:N ratio, (B) $\delta^{13}C_{org}$, (C) concentration of retene, (D) summed concentration of *n*-alkane (ΣALK_{25-31}), (E) summed concentration of branched GDGTs, and (F) crenarchaeol concentration for marine surface sediments. Symbols are as in Fig. 1C. IRD, blue open triangles; soil, red-filled triangles; and coal, green-filled diamonds. The corresponding standard deviations are shown as bars.

Krossfjord IRD (150 μg g_{OC}^{-1}) was lower than that of the average of Kongsfjord IRD (310 μg g_{OC}^{-1}, $n = 3$). The *n*-alkane concentrations in marine sediments ranged from 47 μg g_{OC}^{-1} to 305 μg g_{OC}^{-1} (average = 83 ± 54 μg g_{OC}^{-1}, $n = 29$). These data are plotted in Figs. 2D, 3D.

GDGTs—The concentrations of branched GDGTs, compounds derived from unknown soil bacteria, were between 2 and 16 (average = 8 ± 5 μg g_{OC}^{-1}, $n = 15$), between 5 and 9 (average = 7 μg g_{OC}^{-1}, $n = 4$), and between 1 μg g_{OC}^{-1} and 5 μg g_{OC}^{-1} (average = 3 ± 1 μg g_{OC}^{-1}, $n = 29$) for soils, IRD, and marine sediments, respectively (Figs. 2E, 3E). The crenarchaeol concentrations varied between not detected (i.e., below detection limit) and 5 (average = 0.6 ± 1.2 μg g_{OC}^{-1}, $n = 15$), between 7 and 15 (average = 11 μg g_{OC}^{-1}, $n = 4$), and between 20 μg g_{OC}^{-1} and 350 μg g_{OC}^{-1} (average = 167 ± 69 μg g_{OC}^{-1}, $n = 29$) for soils, IRD, and marine sediments, respectively (Figs. 2F, 3F). The branched GDGTs and crenarchaeol were not detected in the coal samples. The BIT index of Svalbard soils was close to 1, as is typically found for soils (Hopmans et al. 2004; Weijers et al. 2006). BIT values of IRD were much lower and varied between 0.32 and 0.48 (average = 0.4, $n = 4$), while those of marine sediments were generally low and ranged from 0.01 to 0.12 (average = 0.02 ± 0.02, $n = 29$).

Discussion

Contribution of marine OM—The C:N ratio has been widely used to trace sources of OM (marine vs. terrestrial) in Arctic environments (Stein and Macdonald 2004).

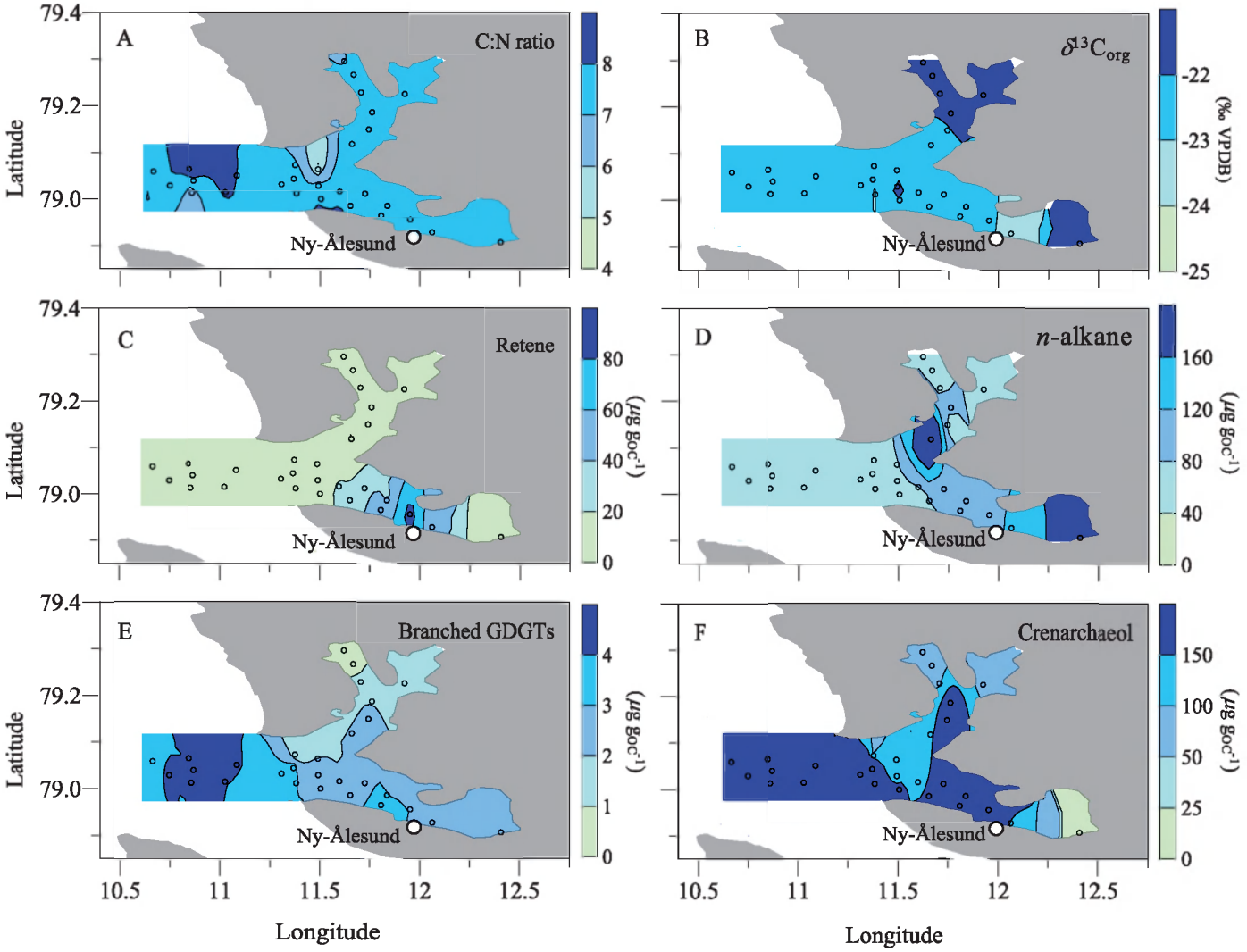

Fig. 3. Spatial distribution pattern of (A) C : N ratio, (B) $\delta^{13}C_{org}$, (C) concentration of retene, (D) summed concentration of *n*-alkane (ΣALK_{25-31}), (E) summed concentration of branched GDGTs, and (F) crenarchaeol concentration in the Kongsfjord–Krossfjord system. The spatial distribution patterns are based on variogram analysis and ordinary kriging (Davis 2002), interpolating the data with $0.2^\circ \times 0.15^\circ$ searching radius. nd indicates 'not detected.'

Higher plant-derived OM is typically characterized by a higher C : N ratio (e.g., > 20; Meyers and Ishiwatari 1993) than that of OM derived from marine organisms (6–9; Müller 1977) because terrestrial OM contains a higher percentage of nonprotein materials. Due to humification and mineralization of plant litter in soils, the C : N ratio of soil OM is typically lower compared to that of vascular plants and varies between 8 and 20 (Hedges and Oades 1997). The C : N ratio of the investigated soils was typically within this range (Fig. 2A). The C : N values of the marine surface sediments (typically 7–8) are indicative for a dominance of marine OM, and showed no specific trend in the spatial distribution pattern (Fig. 3A). Winkelmann and Knies (2005) showed that C : N values of marine surface sediments off Spitsbergen were substantially affected by a contribution of inorganic nitrogen, which accounted for up to 70% of the total nitrogen content. This implies that the relatively low C : N values of marine sediments are possibly, at least in part, due to the high amount of inorganic nitrogen present in fine-grained sediments. However, TOC (wt.%) correlates very well with total nitrogen (wt.%), with a linear relationship and an 0.003 intercept ($r^2 = 0.87$, $n = 36$, $p < 0.001$, data not shown), indicating that the contribution of inorganic nitrogen to the total nitrogen pool is likely negligible in the Krossfjord–Kongsfjord system.

The stable carbon isotope composition of TOC ($\delta^{13}C_{org}$) is another tool widely used for identifying sources of OM (marine vs. terrestrial) in the Arctic realm (Schubert and Calvert 2001; Winkelmann and Knies 2005). The $\delta^{13}C_{org}$ of higher plants that use the Calvin–Benson cycle of carbon fixation (i.e., C_3 plants) ranges from −29.3‰ to −25.5‰, with an average value of about −27‰ (Fry and Sherr 1984; Tyson 1995). A contribution of C_4 plant debris, which is characterized by enriched ^{13}C contents, is unlikely at higher latitudes (Teeri and Stowe 1976). Indeed, the $\delta^{13}C_{org}$ values of soils (on average −26‰) and the coals (on average −25‰) are within the range of C_3 plants, although on the

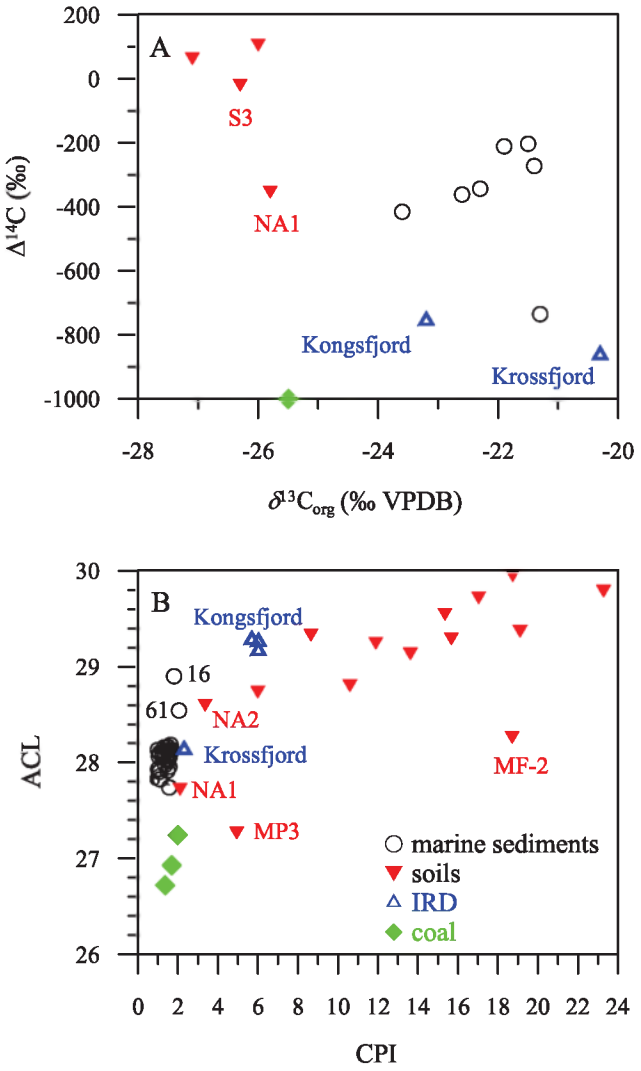

Fig. 4. Scatter-plot of (A) $\delta^{13}C_{org}$ vs. $\Delta^{14}C$ and (B) CPI vs. ACL. Symbols are as in Fig. 1C. *See* also Fig. 1 for the sample positions and names.

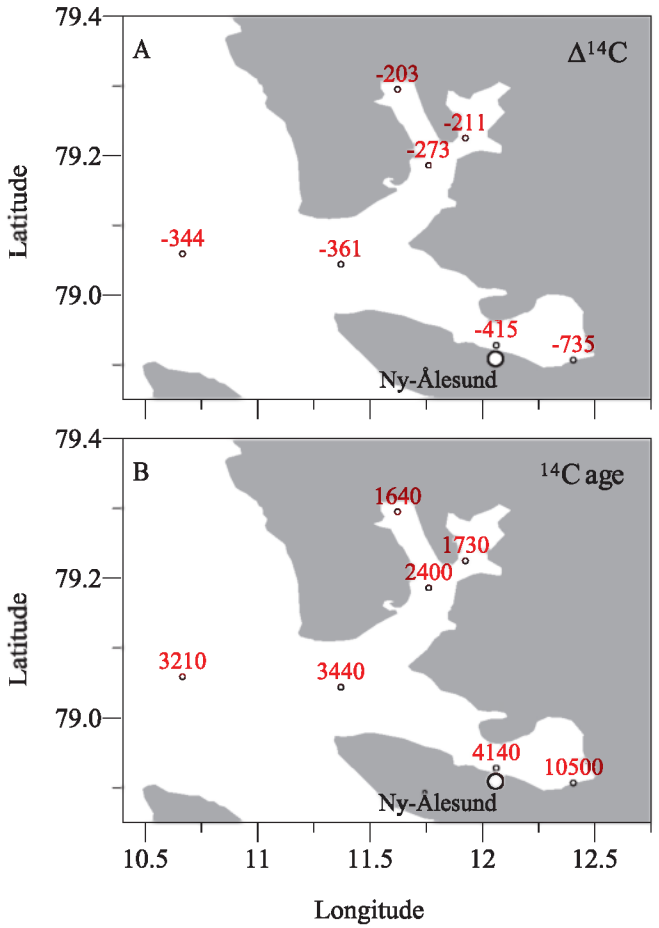

Fig. 5. Spatial distribution pattern of (A) $\Delta^{14}C$ and (B) ^{14}C age in years BP in the Kongsfjord–Krossfjord system.

^{13}C-enriched side. The $\delta^{13}C_{org}$ values of marine sediments are generally more enriched ($> -23‰$; Fig. 2B) in the Kongsfjord–Krossfjord system relative to those of soils and coals, and are indicative of a primarily marine origin ($-20.6‰$) of the sedimentary OM (Winkelmann and Knies 2005).

In contrast, the bulk radiocarbon content ($\Delta^{14}C$ value) of selected marine surface sediments indicates that modern marine OM is not a major contribution to the sedimentary OM (Figs. 4, 5). The carbon dioxide that is used by phytoplankton for marine primary production is only slightly depleted in ^{14}C compared to atmospheric CO_2 (Broecker et al. 1960; Linick 1980) and, therefore, marine surface sediments that predominantly contain marine OM should not be depleted in ^{14}C to a large extent. The additional introduction of radiocarbon in the atmosphere in the fifties and sixties has even resulted in ^{14}C enrichment of marine sedimentary OM and phytoplankton biomarkers in marine surface sediments (Pearson et al. 2000; Smittenberg et al. 2004). The strong depletion in ^{14}C of the marine surface sediments suggests a substantial contribution of ancient OM that is not revealed by the C : N ratio or $\delta^{13}C_{org}$. Below we discuss three potential sources for ancient OM.

Contribution of soil-derived OM—Soils can contain substantial amounts of OM that can be transported to coastal sediments by erosion processes. The turnover time of soil OM is much slower than in marine systems, resulting in preageing (Smittenberg et al. 2006) and, therefore, the input of soil OM can potentially explain the depleted ^{14}C content of the sedimentary OM. However, two lines of evidence, in addition to the C : N ratios or $\delta^{13}C_{org}$ values (*see* above), argue that this is an unlikely source in Svalbard marine sediments. The $\Delta^{14}C$ of OC of two out of four soils showed after-bomb signatures and, thus, modern ages (Fig. 4A), indicating that an input of soil OM cannot be a reason for the depletion in ^{14}C of sedimentary OM. Interestingly, one of the soils (NA1) collected in Ny Ålesund was significantly depleted in ^{14}C but this is likely due to the presence of the coal-derived OM (as discussed below). Our soil data are similar to those by Peterse et al. (2009; i.e., BIT values are close to 1 as a consequence of the generally much higher concentration of branched GDGTs

compared to crenarchaeol). A reliable estimation of the soil OM contribution to sedimentary OM using the BIT index is in part hampered owing to the in-situ production of branched GDGTs in this particular Arctic environment (Peterse et al. 2009). Nevertheless, our results may still be useful for determining soil OM contribution, because basically the BIT end members are still extremely different (i.e., 0.02 for marine sediments and 0.96 for Svalbard soils). Thus, the low BIT values suggest that, in the Kongsfjord–Krossfjord system, the input of soil OM into the fjords is negligible, likely due to the limited soil formation in the cold Arctic environment, which weakens the signature of soil OM in marine environments (Kim et al. 2009*b*; Peterse et al. 2009).

Contribution of coal-derived OM—Coal has been mined in the area around Ny Ålesund in the last century and, therefore, has to be considered as a potential source for ^{14}C-depleted carbon to the sedimentary OM. Coal might have been transported to the fjords through direct coastal erosion or presumably through leaching and/or river run-off. Retene, a higher plant triterpenoid-derived, aromatic compound, appears to be a common dominant component of Svalbard coals (Ćmiel and Fabiańska 2004) and, thus, may be a useful molecular marker for coal-derived OM in marine sediments. High concentrations of retene were, indeed, detected in the coal samples, whereas it was not detectable in all the examined soils except those from around the former coal-mining town Ny Ålesund (NA1 and NA2), which also contained retene in considerable amounts. These two soils (and the anomalous MP3 sample) also show distinct *n*-alkane distributions marked by reduced CPI and ACL values that are more alike than the *n*-alkane distribution of the coals (Fig. 4B). Remarkably, the NA1 soil is also the only soil examined that revealed a significantly reduced Δ^{14}C value (Fig. 5A). Together this indicates that the soils in the proximity of Ny Ålesund contain a substantial contribution of coal-derived OM.

Based on these results, we used retene as a marker for the contribution of coal-derived OM to sedimentary OM. Interestingly, the spatial distribution pattern of the retene concentration indicates relatively high concentrations (up to 14% of that in coal) of retene in the marine sediments of Kongsfjord near Ny Ålesund (Fig. 3C), suggesting a substantial contribution of coal-derived OM similar to the soils around Ny Ålesund. Retene was also detected in the marine sediments in Krossfjord, albeit in much smaller amounts. This implies that (small amounts of) coal might be brought into the fjord system from the Lower Tertiary coal seams. However, the relatively low concentrations in the marine surface sediments other than those in close vicinity of Ny Ålesund (< 10 μg g_{OC}^{-1}; Fig. 3C) indicate that an input of coal-derived OM cannot be primarily responsible for the generally low Δ^{14}C value of the sedimentary OM.

Contribution of IRD-derived OM—The study area is characterised by various glaciers (Fig. 2) and IRD may transport OM from the continent to the marine sediments. Around the Krossfjord basement rocks formed during the Precambrian and the Silurian are predominantly phyllites and mica schist, which were deformed strongly both during the Caledonian orogeny (Silurian) and the Alpidic orogeny (Lower Tertiary; Hjelle 1993). Devonian brownish-red conglomerates and sandstones are exposed in the innermost Kongsfjord and transported by icebergs into the fjord, coloring the IRD red. South of Kongsfjord, Tertiary rocks occur as conglomerates, sandstones, and shales with numerous inter-bedded coal seams (Hjelle 1993). The IRD-derived OM showed highly depleted Δ^{14}C values of -700‰ to -900‰ for Krossfjord and Kongsfjord, respectively (Fig. 4A), indicating that IRD could be a potential contributor of ^{14}C-depleted OM to the sedimentary OM. As indicated by the CPI and ACL values of the *n*-alkanes (Fig. 4B), the Krossfjord IRD contains more mature, Δ^{14}C-depleted OM than the Kongsfjord IRD. The radiocarbon ages of the IRD-derived OM suggest that the IRD likely contained a large contribution of preaged soils formed between the last deglaciation and the neoglaciation ($\sim$ 13,600–4500 yr BP; Svendsen et al. 2002) or possibly a mixture of preaged soils and ancient marine sediments. The latter would explain the relatively low BIT and enriched $\delta^{13}C_{org}$ values of the IRD-derived OM. Interestingly, the marine sediment (NP07-03-61), collected in front of the Kongsvegen glacier at the head of Kongsfjord, had a similar ^{14}C age (10,500 yr BP) compared to that of the Kongsfjord IRD. The BIT value of this sediment (BIT = 0.12; Peterse et al. 2009) was also higher than those of most other marine sediments (≤ 0.02) and it has a summed *n*-alkane concentration (Fig. 3D) and distribution (Fig. 4B) that is close to the Kongsfjord IRD. This supports the idea that the IRD-derived OM input contributed, at least in part, to the Δ^{14}C-depletion of the marine sediments. This input would probably be most significant in front of glaciers but, due to the slow melting of icebergs, could exert its influence on the whole fjord system and beyond.

The C : N values of IRD were typically lower than those of marine sediments. However, the presence of inorganic nitrogen in sediments with high proportions of illite (the clay mineral mainly responsible for ammonium binding) can affect the C : N ratio (Müller 1977; Schubert and Calvert 2001). The C : N values of fine-grained IRD were probably affected by a contribution of inorganic nitrogen because TOC contents were relatively low and, thus, organic nitrogen content was low relative to inorganic nitrogen. Intriguingly, the $\delta^{13}C_{org}$ values of IRD (on average, -22‰) lie much closer to the marine sediments than soils, as would perhaps be expected. The distribution pattern of the $\delta^{13}C_{org}$ values of marine sediments shows slightly more ^{13}C-enriched values closer to the glacier fronts (Fig. 3B). This is opposite to other fjord systems in the Svalbard, which showed a positive gradient from the inner fjords toward marine sites (Winkelmann and Knies 2005). Retene was not detected in IRD and marine sediments collected in front of the glaciers, suggesting no major contributions of coal-derived OM through IRD. Based on these data we surmise that the input of IRD-derived OM is the most logical explanation for the substantial depletion in

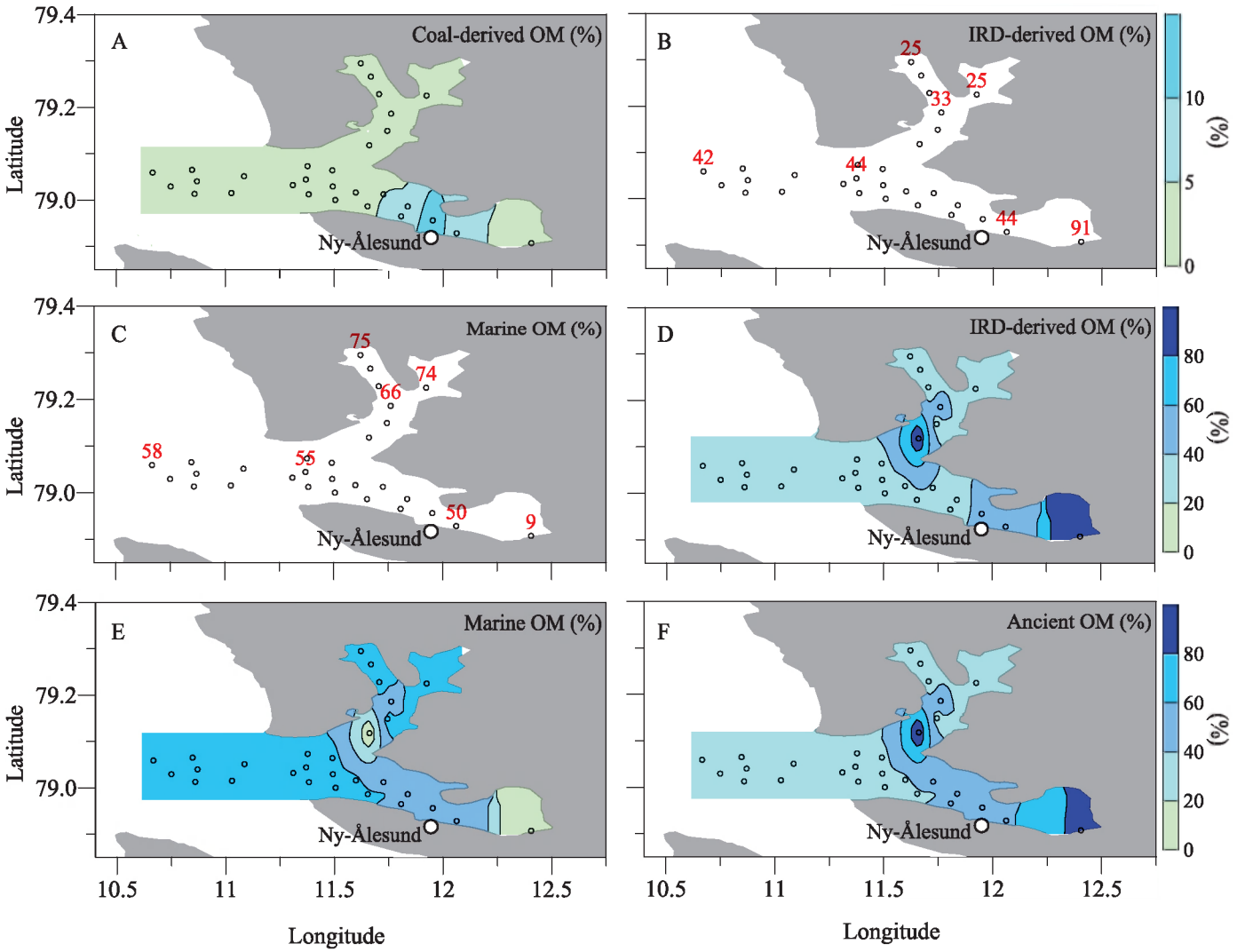

Fig. 6. Spatial distribution pattern of OM sources in the Kongsfjord–Krossfjord system using two different methods. Calculated percentages (%) of (A) coal-derived, (B) IRD-derived, and (C) marine OM to sedimentary OM based on the retene concentration and $\Delta^{14}C$ data (three-end-member mixing model). Calculated percentages (%) of (D) IRD-derived OM, (E) marine OM (the sum of the coal- and IRD-derived OM), and (F) ancient OM to sedimentary OM based on the relationship between the coal-corrected *n*-alkane concentration and the ratio between IRD-derived and marine OM [$F_{IRD} / (F_{IRD} + F_{mar})$; *see* Fig. 7]. The spatial distribution patterns are as in Fig. 3.

^{14}C of sedimentary OM. However, locally, a substantial contribution of coal-derived OM can also be detected.

Mass balance calculations—Quantification of the relative input of terrestrial OM to Arctic marine sediments is usually based on bulk and molecular parameters by means of simplified two end-member mixing models (Schubert and Calvert 2001; Winkelmann and Knies 2005; Belicka and Harvey 2009). However, in general terms this approach is an oversimplification because terrestrial OM brought to the ocean is in nature heterogeneous, containing soil and ancient OM, in addition to contemporary vascular plants (Hedges et al. 1997). The low BIT values in the marine sediments indicate that the soil OM contribution was minor in the Kongsfjord–Krossfjord system but our retene, CPI, ACL, and $\Delta^{14}C$ data suggest the presence of two distinctive ancient OM sources (i.e., coal-derived and IRD-derived OM), which complicates the simple differentiation of marine and terrestrial OM inputs to marine sediments.

We, therefore, estimated relative proportions of marine, coal-derived, and IRD-derived OM to sedimentary OM, combining the retene concentrations with the $\Delta^{14}C$ data for a three end-member mixing model in a similar way as that conducted by Kim et al. (2009*a*):

$$F_{coal} + F_{IRD} + F_{mar} = 1 \quad (4)$$

$$\text{Retene}_{sample} = \text{Retene}_{mar} \times F_{mar} + \text{Retene}_{coal} \times F_{coal} + \text{Retene}_{IRD} \times F_{IRD} \quad (5)$$

$$\Delta^{14}C_{sample} = \Delta^{14}C_{mar} \times F_{mar} + \Delta^{14}C_{coal} \times F_{coal} + \Delta^{14}C_{IRD} \times F_{IRD} \quad (6)$$

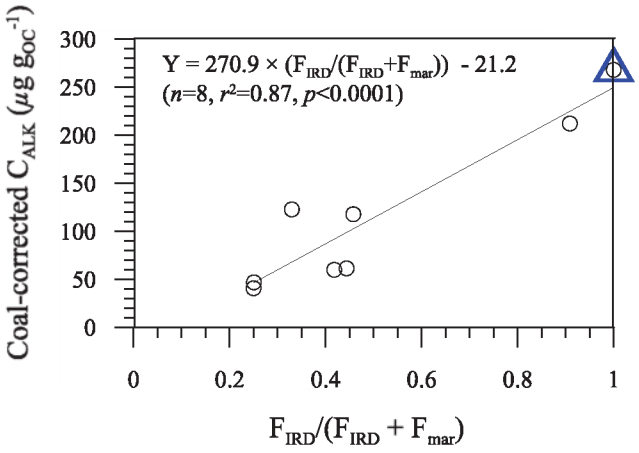

Fig. 7. Correlation of the ratio between IRD-derived and marine OM [F_{IRD} / (F_{IRD} + F_{mar})] obtained from the $\Delta^{14}C$-retene three-end-member mixing model against the coal-corrected *n*-alkane concentrations. The average *n*-alkane concentration value of the Kongsfjord and Krossfjord IRD was used as the IRD end-member value (blue open triangle).

F_{coal}, F_{IRD}, and F_{mar} are the fractions of coal-derived, IRD-derived, and marine OM to sedimentary OM, respectively. The end-member values of retene and $\Delta^{14}C$ are assumed as follows: $Retene_{mar}$ = 0 μg g_{OC}^{-1}, $Retene_{coal}$ = 568 μg g_{OC}^{-1} (the average value of our coal samples), $Retene_{IRD}$ = 0 μg g_{OC}^{-1} (our IRD value), $\Delta^{14}C_{mar}$ = 0‰, $\Delta^{14}C_{coal}$ = −1000‰, and $\Delta^{14}C_{IRD}$ = −809‰ (the average of the IRD values). The percentage of coal-derived OM to sedimentary OM calculated from this method comprised in the range of 0–16% with the highest value close to former coal-mine town Ny Ålesund (Fig. 6A). The calculated IRD-derived OM contribution to sedimentary OM ranged from 25% to 91% with the maximum value in the Kongsvegen glacier front (Fig. 6B). This indicates that most of ancient OM in the Kongsfjord–Krossfjord system was delivered by melting icebergs as mature recycled OM. This three-end-member mixing model suggested that marine OM contributed 9% to 75% to sedimentary OM (Fig. 6C).

Only a few $\Delta^{14}C$ measurements were available; therefore, the above three-component mixing model cannot be used to estimate relative proportions of marine, coal-derived, and IRD-derived OM to sedimentary OM for all surface sediments. In order to better constrain the spatial distribution pattern of IRD-derived OM in the Kongsfjord–Krossfjord system, we investigated if the *n*-alkane concentration in the marine surface sediments instead of ^{14}C values could be used to estimate the ratio between IRD-derived and marine OM. To this end, we first corrected *n*-alkane concentrations (Y; Eq. 7) of marine sediments for local coal contributions:

$$Y = C_{ALK} - (F_{coal} \times C_{ALK}) \quad (7)$$

where C_{ALK} is the summed C_{25} to C_{31} *n*-alkane concentration (ΣALK_{25-31}) of the marine sediments in μg g_{OC}^{-1}. F_{coal} was derived from Eq. (5). Subsequently, the coal corrected *n*-alkane concentrations were correlated against the ratio between IRD-derived and marine OM [F_{IRD} / (F_{IRD} + F_{mar})] for sediments where this ratio could be calculated (i.e., those with ^{14}C data). This resulted in a good linear fit (Fig. 7):

$$Y = 270.9 \times (F_{IRD}/(F_{IRD} + F_{mar})) - 21.2$$
$$(n = 8, r^2 = 0.87, p < 0.0001) \quad (8)$$

This good linear fit suggests that we can use the concentration of coal-corrected ΣALK_{25-31} of the marine sediments to estimate F_{IRD} / (F_{IRD} + F_{mar}) for all marine sediments. The results of these estimates are shown in Fig. 6D,E. This method resulted in slightly lower IRD-derived OM contributions compared to those of the $\Delta^{14}C$-retene three-end-member mixing model. However, the overall spatial distribution pattern was similar with higher IRD-derived OM at the Kongsvegen glacier front. As a result, this three-end-member model resulted in 61% ± 18% of the average marine OM contribution (Fig. 6E) and 39% ± 18% of the average ancient OM contribution (Fig. 6F).

Ancient OM has also been reported as an important OM component in the estuaries of the Great Russian and Canadian–American Arctic Rivers (Guo et al. 2004; Goñi et al. 2005; Drenzek et al. 2007). For example, a coupled molecular isotopic mass balance approach based on compound-specific $\delta^{13}C$ and $\Delta^{14}C$ signatures indicated that about 40–50% of the OM currently being buried on the Canadian Beaufort shelf of the Arctic Ocean was derived from the weathering of ancient sedimentary rocks (Drenzek et al. 2007). Studies on tectonically active margins also showed that small mountainous rivers delivered a substantial amount of ancient OM to the ocean (Komada et al. 2004). Consequently, ancient OM has been efficiently buried on adjacent shelves due to high uplift and erosion rate of ancient sedimentary rock, rapid sediment transport, and slow rate of ancient OM degradation in rivers (Blair et al. 2003). In summary, our results from the Arctic fjord system (Svalbard) support the idea that the reburial of ancient OM in the Arctic Ocean is an important and widespread phenomenon (Blair et al. 2004; Drenzek et al. 2007).

Our results also have implications for the functioning of the benthic food web in the fjords. One of the most important pelagic–benthic coupling processes is the sinking of organic, bio-available matter through the water column to the sea floor, where it can be grazed or buried. At present, there is only scattered information on OM sources contributing to the Kongsfjord–Krossfjord benthic system (*see* overviews in Svendsen et al. 2002). Phytoplankton biomass (i.e., OM from primary production), is an important component of sinking OM and faecal pellets are another source). However, the contribution of ancient OM to sinking OM and, thus, its link to benthic ecosystem functioning and biogeochemical cycling in the benthic layer has not been considered in this Arctic marine system hitherto (Teske et al. 2011). Generally, ancient OM is thought to be much less degradable than fresh marine OM. However, Petsch et al. (2000, 2001) showed that microorganisms enriched from a Late Devonian black-shale weathering profile assimilated ancient OM into their cellular carbon. Hence the role of bacteria and/or eukaryotes capable of utilizing ancient OM as their sole OC source should be taken

into account for the assessment of Kongsfjord–Krossfjord pelagic and benthic ecosystem and, thus, for a better understanding of carbon flows in this ecosystem.

Acknowledgments

We thank two anonymous reviewers for their constructive comments; E. C. Hopmans, J. Ossebaar, and S. Crayford for analytical support; J. A. Godiksen and E. T. Bjørvik for sampling soils at Mitra Peninsula; and A. Eraso and M. C. Dominguez (GLACKMA) for sampling soils near to the Kongsvegen glacier. Thanks also go to N. Koç, other participants, and the crew of the SciencePub International Polar Year cruises on the R/V *Lance* from the Norwegian Polar Institute.

This study was carried out in collaboration with the Norwegian Polar Institute and was supported by a Marie Curie Intra-European Fellowship grant to J.-H. Kim and the European Research Council Project Past Continental Climate Change: Temperatures from Marine and Lacustrine Archives (PACEMAKER).

References

Belicka, L. L., and H. R. Harvey. 2009. The sequestration of terrestrial organic carbon in Arctic Ocean sediments: A comparison of methods and implications for regional carbon budgets. Geochim. Cosmochim. Acta **73:** 6231–6248, doi:10.1016/j.gca.2009.07.020

Benner, R., B. Benitez-Nelson, K. Kaiser, and R. M. W. Amon. 2004. Export of young terrigenous dissolved organic carbon from rivers to the Arctic Ocean. Geophys. Res. Lett. **31:** L05305, doi:10.1029/2003GL019251

Blair, N. E., E. L. Leithold, and R. C. Aller. 2004. From bedrock to burial: The evolution of particulate organic carbon across coupled watershed continental margin systems. Mar. Chem. **92:** 141–156, doi:10.1016/j.marchem.2004.06.023

———, ———, S. T. Ford, K. A. Peeler, J. C. Holmes, and D. W. Perkey. 2003. The persistence of memory: The fate of ancient sedimentary organic carbon in a modern sedimentary system. Geochim. Cosmochim. Acta **67:** 63–73, doi:10.1016/S0016-7037(02)01043-8

Bray, E. E., and E. D. Evans. 1961. Distribution of *n*-paraffin as a clue to recognition of source beds. Geochim. Cosmochim. Acta **22:** 2–15, doi:10.1016/0016-7037(61)90069-2

Broecker, W. S., R. Gerard, M. Ewing, and B. C. Heezen. 1960. Natural radiocarbon in the Atlantic Ocean. J. Geophys. Res. **65:** 2903–2931, doi:10.1029/JZ065i009p02903

Ćmiel, S. R., and M. J. Fabiańska. 2004. Geochemical and petrographic properties of some Spitsbergen coals and dispersed organic matter. Int. J. Coal Geol. **57:** 77–97, doi:10.1016/j.coal.2003.09.002

Cottier, F. R., F. Nilsen, M. E. Inall, S. Gerland, V. Tverberg, and H. Svendsen. 2007. Wintertime warming of an Arctic shelf in response to large-scale atmospheric circulation. Geophys. Res. Lett. **34:** L10607, doi:10.1029/2007GL029948

Davis, J. C. 2002. Statistics and data analysis in geology, 3rd ed. Kansas Geological Survey, John Wiley and Sons.

Dickens, A. F., Y. Gélinas, C. A. Masiello, S. Wakeham, and J. I. Hedges. 2004. Reburial of fossil organic carbon in marine sediments. Nature **427:** 336–339, doi:10.1038/nature02299

Dixon, R. K., S. Brown, R. A. Houghten, A. M. Solomon, C. Trexler, and J. Wisniewski. 1994. Carbon pools and flux of global forest ecosystems. Science **263:** 185–190, doi:10.1126/science.263.5144.185

Drenzek, N. J., D. B. Montluçon, M. B. Yunker, R. W. Macdonald, and T. I. Eglinton. 2007. Constraints on the origin of sedimentary organic carbon in the Beaufort Sea from coupled molecular ^{13}C and ^{14}C measurements. Mar. Chem. **103:** 146–162, doi:10.1016/j.marchem.2006.06.017

Eglinton, G., and R. J. Hamilton. 1963. The distribution of alkanes, p. 187–208. *In* T. Swain [ed.], Chemical plant taxonomy. Academic Press.

Fry, B., and E. B. Sherr. 1984. $\delta^{13}C$ measurements as indicators of carbon flow in marine and freshwater ecosystems. Contrib. Mar. Sci. **27:** 13–47.

Goñi, M. A., M. B. Yunker, R. W. Macdonald, and T. I. Eglinton. 2000. Distribution and sources of organic biomarkers in arctic sediments from the Mackenzie River and Beaufort Shelf. Mar. Chem. **71:** 23–51, doi:10.1016/S0304-4203(00)00037-2

———, ———, ———, and ———. 2005. The supply and preservation of ancient and modern components of organic carbon in the Canadian Beaufort Shelf of the Arctic Ocean. Mar. Chem. **93:** 53–73, doi:10.1016/j.marchem.2004.08.001

Grimalt, J. O., B. R. T. Simoneit, P. G. Hatcher, and A. Nissenbaum. 1988. The molecular composition of ambers. Org. Geochem. **13:** 677–690, doi:10.1016/0146-6380(88)90089-7

Guo, L., and R. W. Macdonald. 2006. Source and transport of terrigenous organic matter in the upper Yukon River: Evidence from isotope ($\delta^{13}C$, $\Delta^{14}C$, and $\delta^{15}N$) composition of dissolved, colloidal, and particulate phases. Glob. Biogeochem. Cycles **20:** GB2011, doi:10.1029/2005GB002593

———, I. Semiletov, O. Gustafsson, J. Ingri, P. Andersson, O. Dudarev, and D. White. 2004. Characterization of Siberian Arctic coastal sediments: Implications for terrestrial organic carbon export. Glob. Biogeochem. Cycles **18:** GB1036, doi:10.1029/2003GB002087

Hedges, J. I., R. G. Keil, and R. Benner. 1997. What happens to terrestrial organic matter in the ocean? Org. Geochem. **27:** 195–212, doi:10.1016/S0146-6380(97)00066-1

———, and J. M. Oades. 1997. Comparative organic geochemistries of soils and marine sediments. Org. Geochem. **27:** 319–361, doi:10.1016/S0146-6380(97)00056-9

Hjelle, A. 1993. The geology of Svalbard. Norsk Polarinstitutt, Oslo.

Hop, H., and others. 2002. The marine ecosystem of Kongsfjorden, Svalbard. Polar Res. **21:** 167–208, doi:10.1111/j.1751-8369.2002.tb00073.x

Hopmans, E. C., S. Schouten, R. D. Pancost, M. T. J. van der Meer, and J. S. Sinninghe Damsté. 2000. Analysis of intact tetraether lipids in archaeal cell material and sediments by high performance liquid chromatography/atmospheric pressure chemical ionization mass spectrometry. Rapid Commun. Mass Spectrom. **14:** 585–589.

———, J. W. H. Weijers, E. Schefuss, L. Herfort, J. S. Sinninghe Damsté, and S. Schouten. 2004. A novel proxy for terrestrial organic matter in sediments based on branched and isoprenoid tetraether lipids. Earth Planet. Sci. Lett. **224:** 107–116.

Huguet, C., E. C. Hopmans, W. Febo-Ayala, D. H. Thompson, J. S. Sinninghe Damsté, and S. Schouten. 2006. An improved method to determine the absolute abundance of glycerol dibiphytanyl glycerol tetraether lipids. Org. Geochem. **37:** 1036–1041, doi:10.1016/j.orggeochem.2006.05.008

———, R. H. Smittenberg, W. Boer, J. S. Sinninghe Damsté, and S. Schouten. 2007. Twentieth century proxy records of temperature and soil organic matter input in the Drammensfjord, southern Norway. Org. Geochem. **38:** 1838–1849, doi:10.1016/j.orggeochem.2007.06.015

Kim, J.-H., R. Buscail, F. Bourrin, A. Palanques, J. S. Sinninghe Damsté, J. Bonnin, and S. Schouten. 2009*a*. Transport and depositional process of soil organic matter during wet and dry storms on the Têt inner shelf (NW Mediterranean). Paleogeogr. Paleoclimatol. Paleoecol. **273:** 228–238, doi:10.1016/j.palaeo.2008.04.019

———, X. Crosta, E. Michel, S. Schouten, J. Duprat, and J. S. Sinninghe Damsté. 2009*b*. Impact of lateral transport on organic proxies in the Southern Ocean. Quat. Res. **71:** 246–250, doi:10.1016/j.yqres.2008.10.005

Komada, K., E. R. M. Druffel, and S. E. Trumbore. 2004. Oceanic export of relict carbon by small mountainous rivers. Geophys. Res. Lett. **31:** L07504, doi:10.1029/2004GL019512

Levin, I., and V. Hesshaimer. 2000. Radiocarbon—a unique tracer of global carbon cycle dynamics. Radiocarbon **42:** 69–80.

Linick, T. W. 1980. Bomb-produced ^{14}C in the surface water of the Pacific Ocean. Radiocarbon **22:** 599–606.

Loeng, H. 1991. Features of the physical oceanographic conditions of the Barents Sea. Polar Res. **10:** 5–18, doi:10.1111/j.1751-8369.1991.tb00630.x

Macdonald, R. W., S. M. Solomon, R. E. Cranston, H. E. Welch, M. B. Yunker, and C. Gobeil. 1998. A sediment and organic carbon budget for the Canadian Beaufort Shelf. Mar. Geol. **144:** 255–273, doi:10.1016/S0025-3227(97)00106-0

Meyers, P. A., and R. Ishiwatari. 1993. Lacustrine organic geochemistry: An overview of indicators of organic matter sources and diagenesis in lake sediments. Org. Geochem. **20:** 867–900, doi:10.1016/0146-6380(93)90100-P

Müller, P. J. 1977. C/N ratios in Pacific deep-sea sediments: Effect of inorganic ammonium and organic nitrogen compounds sorbed by clays. Geochim. Cosmochim. Acta **41:** 765–776, doi:10.1016/0016-7037(77)90047-3

Neff, J. C., J. C. Finlay, S. A. Zimov, S. P. Davydov, J. J. Carrasco, E. A. G. Schuur, and A. I. Davydova. 2006. Seasonal changes in the age and structure of dissolved organic carbon in Siberian rivers and streams. Geophys. Res. Lett. **33:** L23401, doi:10.1029/2006GL028222

Owrid, G., and others. 2000. Spatial variability of phytoplankton, nutrients and new production estimates in the waters around Svalbard. Polar Res. **19:** 155–171, doi:10.1111/j.1751-8369.2000.tb00340.x

Pearson, A., T. I. Eglinton, and A. P. McNichol. 2000. An organic tracer for surface ocean radiocarbon. Paleoceanography **15:** 541–550, doi:10.1029/1999PA000476

Peterse, F., J.-H. Kim, S. Schouten, D. Klitgaard Kristensen, N. Koç, and J. S. Sinninghe Damsté. 2009. Constraints on the application of the MBT/CBT paleothermometer in high latitude environments (Svalbard, Norway). Org. Geochem. **40:** 692–699, doi:10.1016/j.orggeochem.2009.03.004

Petsch, S. T., R. A. Berner, and T. I. Eglinton. 2000. A field study of the chemical weathering of ancient sedimentary organic matter. Org. Geochem. **31:** 475–487, doi:10.1016/S0146-6380(00)00014-0

———, T. I. Eglinton, and J. K. Edwards. 2001. ^{14}C-dead living biomass: Evidence for microbial assimilation of ancient organic carbon during shale weathering. Science **292:** 1127–1131, doi:10.1126/science.1058332

Poynter, J. G., and G. Eglinton. 1990. Molecular composition of three sediments from hole 717C: The Bengal Fan, p. 155–161. *In* J. R. Cochran and D. A. V. Stow [eds.], Proceedings of the Ocean Drilling Program, Scientific Results 116: Ocean Drilling Program, College Station, Texas.

Schouten, S., C. Huguet, E. C. Hopmans, M. V. M. Kienhuis, and J. S. Sinninghe Damsté. 2007. Analytical methodology for TEX_{86} paleothermometry by high-performance liquid chromatography/atmospheric pressure chemical ionization-mass spectrometry. Anal. Chem. **79:** 2940–2944, doi:10.1021/ac062339v

Schubert, C. J., and S. E. Calvert. 2001. Nitrogen and carbon isotopic composition of marine and terrestrial organic matter in Arctic Ocean sediments: Implications for nutrient utilization and organic matter composition. Deep-Sea Res. Part I **48:** 789–810, doi:10.1016/S0967-0637(00)00069-8

Simoneit, B. R. T., J. O. Grimalt, T. G. Wang, R. E. Cox, P. G. Hatcher, and A. Nissenbaum. 1986. Cyclic terpenoids of contemporary resinous plant detritus and of fossil woods, ambers and coal. Org. Geochem. **10:** 877–889, doi:10.1016/S0146-6380(86)80025-0

Smittenberg, R. H., T. I. Eglinton, S. Schouten, and J. S. Sinninghe Damsté. 2006. Ongoing buildup of refractory organic carbon in boreal soils During the Holocene. Science **314:** 1283–1286, doi:10.1126/science.1129376

———, E. C. Hopmans, S. Schouten, J. M. Hayes, T. I. Eglinton, and J. S. Sinninghe Damsté. 2004. Compound-specific radiocarbon dating of the varved Holocene sedimentary record of Saanich Inlet, Canada. Paleoceanography **19:** PA2012, doi:10.1029/2003PA000927

Stein, R., and R. W. Macdonald. 2004. The organic carbon cycle in the Arctic Ocean. Springer.

Stuiver, M., and H. A. Polach. 1977. Discussion reporting of ^{14}C data. Radiocarbon **19:** 355–363.

Svendsen, H., and others. 2002. The physical environment of Kongsfjorden–Krossfjorden, an arctic fjord system in Svalbard. Polar Res. **21:** 133–66, doi:10.1111/j.1751-8369.2002.tb00072.x

Teeri, J. A., and L. G. Stowe. 1976. Climatic patterns and the distribution of C4 grasses in North America. Oecologia **23:** 1–12.

Teske, A., A. Durbin, K. Ziervogel, C. Cox, and C. Arnosti. 2011. Microbial community composition and function in permanently cold seawater and sediments from an Arctic fjord of Svalbard. Appl. Environ. Microbiol. **77:** 2008–2018, doi:10.1128/AEM.01507-10

Tyson, R. V. 1995. Sedimentary organic matter: Organic facies and palynofacies. Chapman and Hall.

van Dongen, B. E., I. Semiletov, J. W. H. Weijers, and Ö. Gustafsson. 2008. Contrasting lipid biomarker composition of terrestrial organic matter exported from across the Eurasian Arctic by the five great Russian Arctic rivers. Glob. Biogeochem. Cycles **22:** GB1011, doi:10.1029/2007GB002974

Walsh, E. M., A. E. Ingalls, and R. G. Keil. 2008. Sources and transport of terrestrial organic matter in Vancouver Island fjords and the Vancouver–Washington Margin: A multiproxy approach using $\delta^{13}C_{org}$, lignin phenols, and the ether lipid BIT index. Limnol. Oceanogr. **53:** 1054–1063, doi:10.4319/lo.2008.53.3.1054

Weijers, J. W. H., S. Schouten, O. C. Spaargaren, and J. S. Sinninghe Damsté. 2006. Occurrence and distribution of tetraether membrane lipids in soils: Implications for the use of the TEX_{86} proxy and the BIT index. Org. Geochem. **37:** 1680–1693, doi:10.1016/j.orggeochem.2006.07.018

Wiencke, C. 2004. The coastal ecosystem of Kongsfjorden, Svalbard. Synopsis of biological research performed at the Koldewey Station in the years 1991–2003. Ber. Polarforsch. Meeresforsch. **492:** 1–244.

Winkelmann, D., and J. Knies. 2005. Recent distribution and accumulation of organic carbon on the continental margin west off Spitsbergen. Geochem. Geophys. Geosyst. **6:** Q09012, doi:10.1029/2005GC000916

Yunker, M. B., R. W. Macdonald, D. J. Veltkamp, and W. J. Cretney. 1995. Terrestrial and marine biomarkers in a seasonally ice-covered Arctic estuary: Integration of multivariate and biomarker approaches. Mar. Chem. **49:** 1–50, doi:10.1016/0304-4203(94)00057-K

Associate editor: Peter Hernes

Received: 06 September 2010
Accepted: 07 March 2011
Amended: 11 May 2011